Two-dimensional lattice liquids

Santi Prestipino*
Istituto Nazionale per la Fisica della Materia (INFM), Italy
and International School for Advanced Studies (SISSA), via Beirut 2-4, I-34013 Trieste, Italy
(Received 2 February 2000)

Evidence is presented, based on transfer-matrix and Monte Carlo calculations, for the occurrence of a gas-liquid phase transition in suitably constructed, two-dimensional lattice-gas models with extended hard-core repulsion on the triangular lattice. Three different models having this property are identified. The first system is characterized by nearest-neighbor exclusion and an interparticle attraction ranging from second- to fourth-neighbor distance. In a further example, the hard core reaches second neighbors, while the attraction ranges from third to fifth neighbors. Finally, in a third model, the core extends up to fourth neighbors, while the attraction covers all distances from fifth to eighth neighbors. I discuss how to use these results in order to make a realistic lattice simulation of the triangular, (111) surface of a fcc solid.

PACS number(s): 05.70.Ce, 61.20.Gy, 61.20.Ja, 64.70.Dv

I. INTRODUCTION

In the late 1960s, an important issue in statistical mechanics was to understand the phase behavior of two-dimensional (2D) lattice gases of hard-core particles [1]. At that time, the development of computer architectures with enough memory and computing power made it possible for the first time to investigate, by the transfer-matrix method, the phase diagram of rather complex 2D lattice systems. The main purpose of these studies was to bridge the gap existing between the phase behavior of elementary Ising-like lattice gases, which undergo just a single transition [2], and the behavior of continuous hard-particle systems which, in 3D, are generally found in three phases, i.e., solid, liquid, and gas. After a burst of interest that lasted a few years, this area was apparently abandoned and, in the last three decades, most of the effort has been directed toward an understanding of the mechanisms of 2D melting/freezing in continuous systems, especially in the light of the possible existence of a hexatic phase [3].

The first model of a 2D homogeneous and isotropic lattice gas with a phase diagram containing a solid, a liquid, and a gas phase was given by Orban *et al.* [4]. In this model, which is defined on the square lattice, hard-core exclusion extends up to third neighbors, while fourth- and fifth-neighbor particles experience a mutual attraction. Later, this model was used as a tool for investigating various issues in surface physics [5]. To the best of my knowledge, no other model of this kind was found until very recently Poland, using series expansions and the Bethe approximation, has presented evidence of similar phase behavior in a 2D lattice-gas system defined on the hexagonal lattice [6].

From all of these studies, it has become clear that the standard three phases are stable on a lattice as long as (a) the core region encompasses, in addition to the central site, also a number of neighbor sites, and (b) the attractive interaction outside the core is rather extended as well. If condition (a) holds but (b) does not, a single first-order phase transition is generally found from a gaseous low-density phase to a solid high-density phase, possibly turning continuous at high temperature. In this case, the problem is to reintroduce the *liquid* phase. I note that, when condition (a) is not fulfilled (i.e., exclusion is limited to the central site), it is the solid that is washed out and, no matter how long is the range of attraction, there is only one phase transition left of the gas-liquid type [6,2].

In the 3D continuum, the situation is, in many respects, similar. In particular, the spherically symmetric square-well potential

$$V(r)=\begin{cases} +\infty & \text{for } r<\sigma \\ -\epsilon & \text{for } \sigma<r<\sigma+\delta \\ 0 & \text{for } r>\sigma+\delta \end{cases} \tag{1}$$

is known to undergo a gas-liquid transition only provided that $\delta/\sigma \gtrsim 1/3$ [7]. It would be useful to have a simple criterion like this in 2D also.

As yet, no 2D lattice model whose behavior is reminiscent of, say, argon has been reported on the triangular lattice. Here, I will fill this gap by showing that, within the class of models whose solid phase is of a triangular symmetry, the three simplest lattice gases with a stable liquid phase are (see Fig. 1) (1) a model with nearest-neighbor exclusion and second-, third-, and fourth-neighbor interparticle attraction; (2) a model where the hard-core region covers first and second neighbors, while particles that are third, fourth, or fifth neighbors attract each other; (3) a model where any neighbor site of a particle up to fourth neighbors is forbidden, while the attraction ranges from fifth- up to eighth-neighbor distance.

Finding ''realistic'' lattice models in 2D is certainly interesting for academic or pedagogical reasons, but also with the view of constructing a sufficiently simple 3D lattice gas whose surface may resemble that of a continuum model. In fact, there are phenomena occurring at the surface of a 3D solid that show a delicate interplay between discrete and continuous degrees of freedom, like, for instance, the early stages of surface melting. The study of such phenomena can

*Email address: prestip@sissa.it

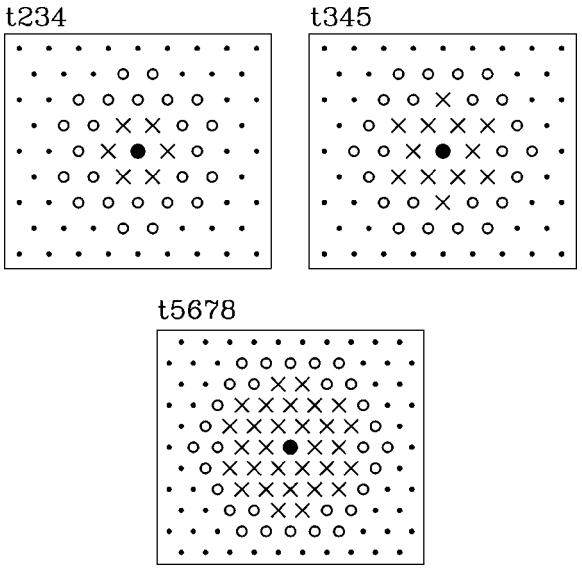

FIG. 1. The three lattice-gas models that are the subject of the present paper. Each of them has a stable liquid phase (see Sec. III). In each panel, excluded sites ($\times$) and attractive sites ($\bigcirc$) are shown separately. Attraction reaches fourth neighbors in the t234 model, fifth neighbors in the t345 model, and eighth neighbors in the t5678 model. In all cases, no interaction is felt beyond this distance (black dots). For these models, the ratio between the upper cutoff of the potential and the core radius is smaller for larger core size. In particular, it is $\sqrt{7}$ for the t234 model, $\sqrt{3}$ for the t345 model, and $4/\sqrt{7}$ for the t5678 model.

benefit greatly from the simulation of a lattice system with three phases in a layer. I shall present below a 3D lattice gas that is aimed at reproducing the entire thermal evolution of the (111) facet of a rare-gas solid at equilibrium, including the preroughening transition of the solid-vapor interface [8], the concurrent onset of surface melting [9], up to roughening and the growth of a thick liquid film between the solid and the vapor.

This paper is organized as follows. In Sec. II, after a reconsideration of former results for the square and hexagonal lattices, a general homogeneous and isotropic lattice-gas model is introduced, and the method used in order to work out its phase diagram is carefully outlined. Then, in Sec. III, selected cases are analyzed, where there is sharp evidence both from the transfer matrix and from Monte Carlo simulation, of a three-phase behavior. Next, in Sec. IV, I discuss how to define a 3D lattice gas having three phases in a layer also. Further remarks and future perspectives are left to the Conclusions.

II. MODEL AND METHOD

I hereby consider statistical systems of indistinguishable ''particles'' existing on the $\mathcal{N}$ sites of a regular 2D lattice. Multiple site occupancy is forbidden, so that occupation numbers c_i can be either 0 or 1 ($i=1,\ldots,\mathcal{N}$). The interaction between two particles is assumed to be hard-core repulsive at short distances, while being attractive outside the core region, at least up to a certain cutoff. As a result, the (strictly pairwise) Hamiltonian of the system takes the form $H=\Sigma_{i<j}V(|i-j|)c_ic_j$, with $V(|i-j|)=+\infty$ if simultaneous occupation of sites i and j is forbidden, whereas $V(|i-j|)<0$ within the range of distances where the interaction is attractive. It is well known that a large-distance attraction between the particles is a necessary, albeit not sufficient, condition for having a well-defined gas-liquid phase transition.

It is my intention here to find the simplest lattice gases with a solid, a liquid, and a gas phase on the triangular lattice, under the condition that the solid phase is triangular as well. The simplest case is when hard-core exclusion is limited to first-neighbor sites only. In this case, the closest-packing density $\rho_{\max}=1/3$. A second case is when both first and second neighbors of an occupied site are forbidden, which leads to a maximum number density of 1/4. A further possibility is to exclude up to fourth-neighbor sites ($\rho_{\max}=1/9$). Upon supplying each of these hard-core potentials with a suitably long-ranged attractive tail, it should be possible to obtain a stable liquid in all of the three cases above.

In order to keep notation as short as possible, the acronym t34 is used for a *triangular* lattice model where third- and fourth-neighbor sites are attractive, while first- and second-neighbor sites of a particle are forbidden, and so forth. For instance, the model by Orban *et al.* will be referred to as the s45 model (''s'' standing for *square*), whereas Poland's model is here named the h23 model (''h'' after *hexagonal*). In the following section, I shall provide sharp evidence of three phases in the t234 model, in the t345 model, and in the t5678 model (Fig. 1). In each of these cases, a shorter range of attraction between the particles seemed insufficient to stabilize the liquid phase.

Coming to the method, I use both transfer-matrix (TM) and grand-canonical Monte Carlo (MC) methods. The TM approach [10] to the statistical mechanics of a lattice system has a long tradition. If the interaction range is sufficiently short, the exact free energy of a system, being infinite in one spatial direction and finite in the other(s), can be computed as the logarithm of the maximum eigenvalue of a (transfer) matrix. In 2D, the simplest case is when this matrix encodes the interaction between a row of sites and the next row along the infinite strip direction y. In this case, the matrix size equals the total number of states in a row. More generally, depending on the interaction range, the natural lattice unit (NLU) can consist of just a single row, or a pair of consecutive rows, or a triplet of rows, etc. Upon increasing the number N_x of sites in a row, phase-transition signatures gradually emerge, thus allowing one to extract the infinite-size behavior by scaling arguments. The virtue of the TM method is limited only by the range of the potential used and by the core extension, which determine in turn what is the maximum x size that can be stored in the computer.

It was Runnels that pioneered the use of the TM technique in the study of 2D lattice gases [11,12]. He and his coworkers were the first to provide a breakthrough in the computational simplification of the problem, by showing how it is possible, using symmetry arguments, to reduce the TM size substantially without affecting the maximum eigenvalue λ_1, which is the one controlling the grand canonical pressure (i.e., the grand potential) of the infinite strip:

$$P=\frac{k_BT}{\mathcal{N}_{\mathrm{NLU}}}\ln\lambda_1, \tag{2}$$

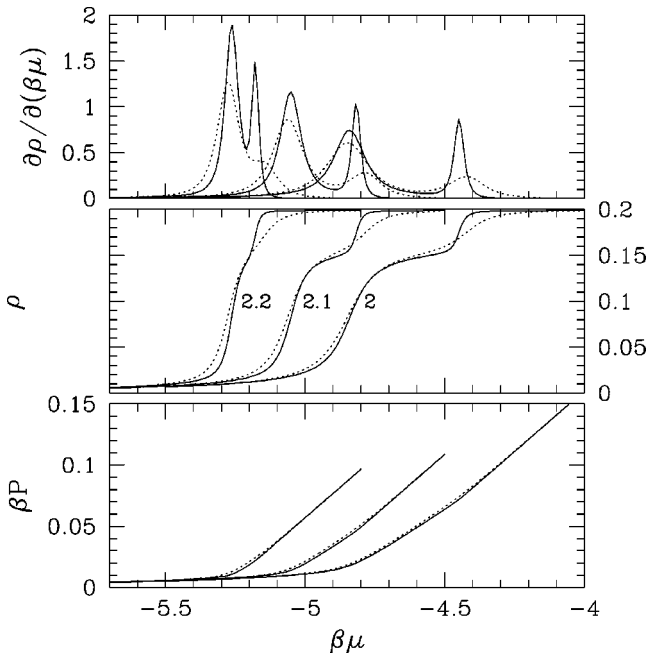

FIG. 2. TM results for the s45 model of Sec. III A. Data are shown for two strip sizes, 10 (dotted line) and 15 (continuous line), and for three isotherms, $\beta\epsilon=2,2.1,2.2$. From top to bottom, results for the reduced compressibility $\partial\rho/\partial(\beta\mu)$, the average density ρ, and the reduced pressure βP are shown. Two peaks in each compressibility curve give the proof of the existence of three phases in this model.

where T is the temperature and $\mathcal{N}_{\mathrm{NLU}}$ is the number of sites in the NLU. In particular, in the square-lattice case, row states can be grouped into equivalence classes bringing together states that map onto each other upon a translation along x and/or a reflection with respect to the strip axis. Then, a matrix that is a condensed form of the TM can be defined, of size equal to the number of equivalence classes, whose maximum eigenvalue is the same as for the original TM. I refer to [11,12] for further details. It is only worth mentioning here that, in the triangular-lattice case, when the x and the y axis are both oriented along nearest-neighbor-bond directions, the group of symmetry transformations includes, besides translations along x, also reflections with respect to an axis perpendicular to x, passing through the center of the bottom row in the NLU.

I have complemented the TM study with Metropolis MC data in the grand canonical ensemble (temperature T and chemical potential μ being the control parameters). Typically, three million MC sweeps are produced for $L\times L$ lattices of increasing size, up to a maximum of $L=60$, with periodic boundary conditions. I choose the x and the y axis along two neighbor-bond directions forming an angle of 120°. A MC sweep here consists of one average attempt per site to change the occupation number from c to $1-c$. Occasionally also the Kawasaki type of moves are considered; see Sec. III E below. For fixed values of $\beta\equiv(k_BT)^{-1}$ and $\beta\mu$, various quantities are computed: (1) the number density $\rho=\langle N\rangle/L^2$, $N=\Sigma_i c_i$ being the current particle number; (2) the average energy $U=\langle H\rangle$; (3) the isothermal compressibility $K_T=\rho^{-2}(\partial\rho/\partial\mu)_T$; and (4) the specific heat at constant chemical potential, $C_\mu=TL^{-2}(\partial S/\partial T)_\mu$. In particular, the latter two quantities are expressed in terms of grand canonical averages as follows:

$$\rho k_BTK_T=\frac{\langle(\Delta N)^2\rangle}{\langle N\rangle}; \tag{3}$$

$$C_\mu=\frac{k_B}{L^2}[\beta^2\langle(\Delta H)^2\rangle+(\beta\mu)^2\langle(\Delta N)^2\rangle - 2\beta\times\beta\mu(\langle HN\rangle-\langle H\rangle\langle N\rangle)], \tag{4}$$

where $\Delta N=N-\langle N\rangle$ and $\Delta H=H-\langle H\rangle$. Note that $C_\mu>0$, owing to the fact that the grand potential is a concave function of T.

As a rule, simulation runs are carried out in sequence, starting from the empty lattice at a very low $\beta\mu$, and then increasing it progressively. After the run at a given $\beta\mu$ has been completed, the last configuration obtained is taken as the starting point of the next run at a slightly larger $\beta\mu$ value. Likewise, other runs are performed on the solid side of the phase diagram, starting from a perfect crystal at a high enough $\beta\mu$, which is then reduced step by step. By such a

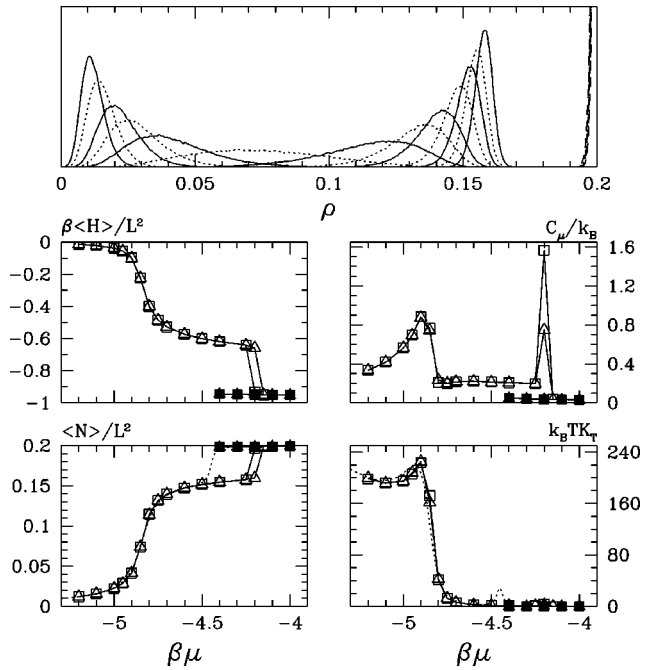

FIG. 3. MC data for the s45 model of Sec. III A, along the isotherm $\beta\epsilon=2$. Above: density histograms for a number of $\beta\mu$ values ranging from -5.2 to -4 (the lattice is 40×40). In particular, a dashed line is used for each run of a sequence starting, at $\beta\mu=-4$, from a perfect crystal configuration. Units along the y axis are arbitrary. Below: thermodynamic quantities (exact results for a strip of 15 sites are also reported as a dotted line). Two lattice sizes are compared, $L=30$ ($\triangle$) and $L=40$ ($\square$). Values of $\beta\mu$ here are the same as those used for the histograms above. All data points are affected by an error that is smaller in magnitude than the size of the symbols. Full markers refer to simulation runs of the sequence starting on the solid side of the phase diagram. While the transition from the gas to the liquid is very smooth (no singularity apparently occurs in the thermodynamic potential), the liquid-solid transition is sharply discontinuous (with liquid undercooling and hysteresis).

method, and provided $\beta\mu$ is increased in small enough steps, one makes the entrapment of the system into a metastable glassy configuration more unlikely to occur at moderate densities. In fact, this would be a more likely outcome if, at any $\beta\mu$, the run were always started from the empty lattice.

Within the above setup, when freezing happens to be discontinuous, undercooling of the liquid is generally observed (usually, overheating of the solid is not obtained). This means that, in the region of liquid-solid coexistence, thermodynamic quantities are sensitive to whether the run was started from a liquidlike or a solidlike configuration (hysteresis).

Finally, a useful tool when studying the phase behavior of a lattice-gas system is to monitor, e.g., at a given β, the evolution of the MC density histogram as a function of μ. In a finite system, a roughly Gaussian peak in this histogram is the imprint of a homogeneous phase, while phase coexistence appears as a bimodal density distribution. Hence, insofar as a liquid region is present in the phase diagram, it will be possible to discriminate between smooth and first-order condensation just from looking at the evolution of the density histogram.

III. RESULTS

A. Model s45

First, I reconsider the model of Ref. [4] since it is paradigmatic of the behavior of a three-phase lattice gas. This is a square-lattice model with hard-core exclusion up to third neighbors, whereas fourth- and fifth-neighbor particles attract each other with a strength of $\epsilon_4=-1.2\epsilon$ and $\epsilon_5=-\epsilon$, respectively ($\epsilon>0$). Within the TM framework, the problem is to enumerate all the states of two consecutive strip rows. After symmetry reduction, the leading eigenvalue of the compressed TM is computed by an iterative method that is far more efficient than full matrix diagonalization. Density and compressibility are evaluated from the raw βP data as a three-point numerical first- and second-order derivative, respectively ($\beta\mu$ is increased by 0.01 at a time). As a rule, the number of iterative steps that are necessary to bring the maximum TM eigenvalue to convergence is larger the larger is the $\beta\mu$ derivative of the density.

In Fig. 2, I show results for $N_x\times\infty$ strips of two sizes, $N_x=10$ and 15 (note that the square solid of density $\rho=1/5$ fits exactly into the strip provided N_x is a multiple of 5). The data of Fig. 2 are relative to three distinct isotherms, $\beta\epsilon=2$, 2.1, and 2.2. For $N_x=15$, the two-row states are 9327 in total, while the number of equivalence classes is just 353. From Fig. 2, it is clear that three different phases exist. This is manifested by the existence of two steps in the density plot, which are the fingerprint of gas-liquid and liquid-solid coexistence, or equivalently by the two peaks in $\partial\rho/\partial(\beta\mu)$, a quantity that is proportional to the isothermal compressibility. By the way, a peak in this derivative is not necessarily connected with a second-order transition. When the system is finite, a compressibility peak may also allude to a first-order transition or it could be simply the result of crossing a disorder line. Only a scaling study of the peak height can definitely settle this question, allowing one to distinguish unambigously between the above three cases [1].

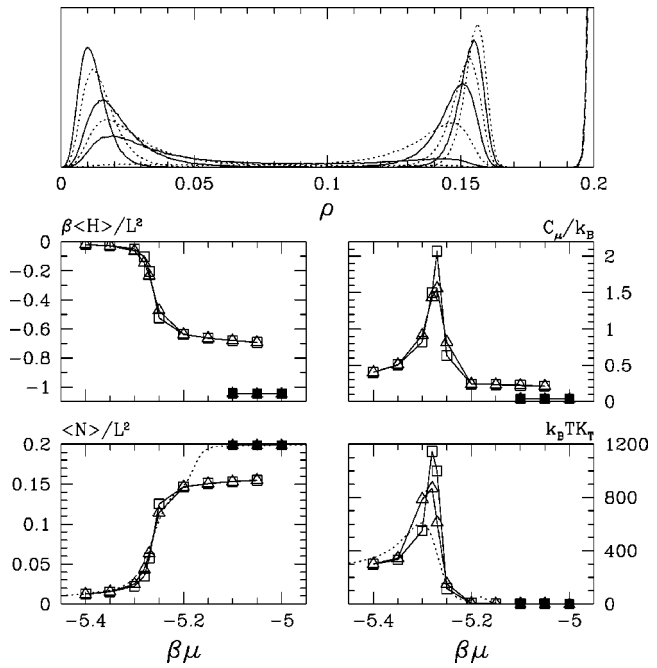

FIG. 4. MC data for the s45 model of Sec. III A, along the isotherm $\beta\epsilon=2.2$. Above: density histograms for a number of $\beta\mu$ values ranging from -5.4 to -5 (the lattice is 40×40). In particular, a dashed line is used for each run of a sequence starting, at $\beta\mu=-5$, from a perfect crystal configuration. Units along the y axis are arbitrary. Below: thermodynamic quantities (exact results for a strip of 15 sites are also reported as a dotted line). Two lattice sizes are compared, $L=30$ ($\triangle$) and $L=40$ ($\square$). Values of $\beta\mu$ here are the same as for the histograms above. All data points are affected by an error that is smaller in magnitude than the size of the symbols. Full markers refer to simulation runs of the sequence starting on the solid side of the phase diagram. Both transitions here, gas-liquid and liquid-solid, are very sharp.

The TM results have been checked by MC simulations. In Figs. 3 and 4, I show simulation data for two isotherms, $\beta\epsilon=2$ and 2.2. Two lattice sizes were considered, $L=30$ and $L=40$. Density histograms and thermodynamic quantities show in a rather convincing way that a liquid phase exists in the same $\beta\mu$ interval as suggested by the TM study, the liquid density being about 80% of the closest-packing density. Moreover, the transition from gas to liquid is smooth for $\beta\epsilon=2$ (Fig. 3), while it is first order for $\beta\epsilon=2.2$ (Fig. 4). Probably no gas-liquid transition line is crossed when $\beta\epsilon=2$, since K_T and C_μ show only a poor size dependence. Finally, the phase transition to the solid is always first order and accompanied by hysteresis.

B. Model h23

I have TM results also for the three-phase model of Poland [6]. This is a hexagonal-lattice model where the interaction range reaches third neighbors. Two different cuts of the hexagonal lattice are considered here; hence strips of two kinds. In one case, two sites being consecutive along the infinite, y direction of the strip are first neighbors of each other (a strip); in the other case, a nearest-neighbor pair is formed by any two consecutive sites along x (b strip). In an a strip, couplings exist between a site of the strip and others that lie two rows further along, whereas horizontal interac-

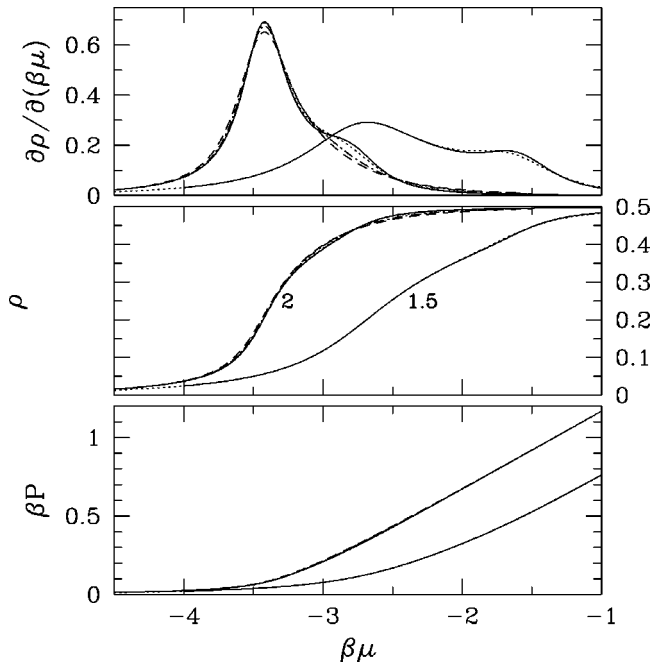

FIG. 5. TM results for the h23 model of Sec. III B. Data are shown for an *a* strip of two sizes, 8 (dotted line) and 10 (continuous line), and for two isotherms, $\beta\epsilon=1.5$ and 2. For the latter, data points for *b* strips are also reported ($N_x=8$, dashed line; $N_x=10$, dot-dashed line). From top to bottom, results for the reduced compressibility, the average density, and the reduced pressure are shown. The TM evidence for the liquid is less obvious in this case than in the s45 model (Fig. 2). In any case, this evidence is stronger for *a* strips than for *b* strips.

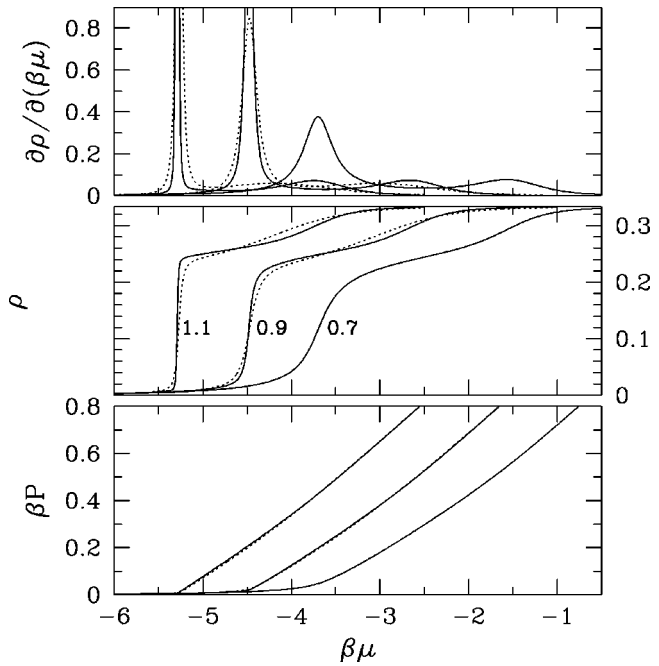

FIG. 6. TM results for the t234 model of Sec. III C. Data are shown for two strip sizes, 6 (dotted line) and 9 (continuous line), and for three isotherms, $\beta\epsilon=0.7,0.9,1.1$. From top to bottom, results for the reduced compressibility, the average density, and the reduced pressure are shown. The overall structure of the reduced compressibility is suggestive of the existence of a liquid phase spreading over a rather wide density interval.

tions are nearest neighbor only; it is the other way around in the case of a *b* strip, where a row is coupled only with the next row along *y* and next-nearest-neighbor *x* interactions are present. In both cases, the NLU is made of two rows and N_x is even. Symmetry transformations of the strip are *x* translations of an even number of sites and parity-conserving reflections, i.e., $(i,j)\rightarrow(N_x+2-i,j)$, (i,j) being the integer coordinates of the generic site. For $N_x=10$, which is our maximum strip size, the number of states is originally 15127 for an *a*-strip, while the number of equivalence classes is only 1543 (for a *b*-strip, the same numbers are 10508 and 1220, respectively).

I use the same parameters as in Ref. [6], i.e., $\epsilon_2=-5\epsilon/9$ and $\epsilon_3=-\epsilon$. From Poland's study, the triple point is expected at $\beta\epsilon\simeq 2.57$ and $\beta\mu\simeq -4.28$. However, if we stay too close to the triple point and the strip width is small, condensation and solidification cannot be disentangled and a single density jump will be observed. Hence, values of $\beta\epsilon$ that are far enough from 2.57 must be considered (not too small, however). In Fig. 5, results are shown for an *a* strip at $\beta\epsilon=1.5$ and 2. For $\beta\epsilon=2$, I show also data for *b* strips. When $\beta\epsilon=1.5$, the $\beta\mu$ derivative of the density has two maxima: this gives us the clue that the liquid is indeed present. However, at this temperature, the gas-liquid ''transition'' associated with the higher peak could just be the crossing of a disorder line. For $\beta\epsilon=2$, the liquid-solid peak becomes the hump of the other peak, while even this feature is missing in the curves relative to *b* strips. Clearly, more information can be obtained from a systematic MC study of the h23 model, which, however, was not attempted here. Nonetheless, I checked at least in a number of cases by MC that the TM calculations were done correctly.

C. Model t234

After having checked my computer programs successfully against known cases, I move to the triangular lattice. First, I consider t2 . . . models. By a series of trial calculations, I convinced myself that no liquid is present in the t2 model, nor in the t23 model. In fact, I was never able to observe, at least within the maximum strip size that I could handle numerically, two distinct peaks in the reduced compressibility as a function of $\beta\mu$. Therefore, I jump directly to the t234 model.

For $\epsilon_2=-1.5\epsilon$, $\epsilon_3=-1.2\epsilon$, and $\epsilon_4=-\epsilon$, I plot in Fig. 6 TM results for two strip sizes ($N_x=6$ and 9) and for three isotherms ($\beta\epsilon=0.7$, 0.9, and 1.1). N_x must be a multiple of 3 in order that the triangular solid (of density $\rho=1/3$) fits exactly into the strip. Given the long potential range, three-row states must be counted in this case. For $N_x=9$, the original TM size is 23 131; after collecting states into equivalence classes, this number eventually becomes 1392. The characteristic two compressibility peaks of a three-phase system are observed for any $\beta\epsilon$ in the interval 0.5–1.1. Surprisingly, condensation appears to be sharper than solidification. As temperature goes down, the condensation line moves slowly toward the solidification line until, at the triple point, the two lines merge together into a single gas-solid transition line.

I also ran a MC program of this model for $\beta\epsilon=0.9$. After equilibration, two million MC sweeps were produced for two sizes, $L=24$ and $L=36$ (see Fig. 7). Density histograms and

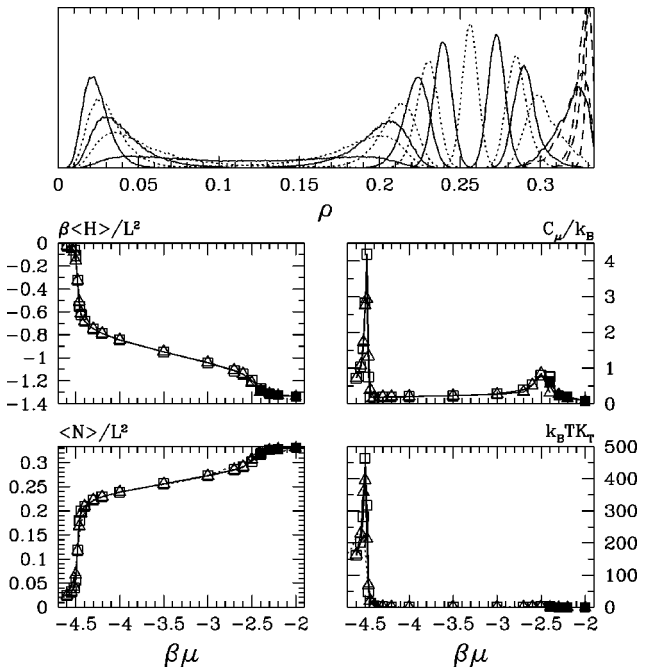

FIG. 7. MC data for the t234 model of Sec. III C, along the isotherm $\beta\epsilon=0.9$. Above: density histograms for a number of $\beta\mu$ values ranging from -4.6 to -2 (the lattice is 36×36). In particular, a dashed line is used for each run of a sequence starting, at $\beta\mu=-2$, from a perfect crystal configuration. Units along the y axis are arbitrary. Below: thermodynamic quantities (exact results for a strip of 9 sites are also reported as a dotted line). Two lattice sizes are compared, $L=24$ ($\triangle$) and 36 ($\square$). Values of $\beta\mu$ here are the same as for the histograms above. All data points are affected by an error that is smaller in magnitude than the size of the symbols. Full markers refer to simulation runs of the sequence starting on the solid side of the phase diagram. While the gas-liquid transition is very sharp, the liquid-solid transition is at most weakly first order.

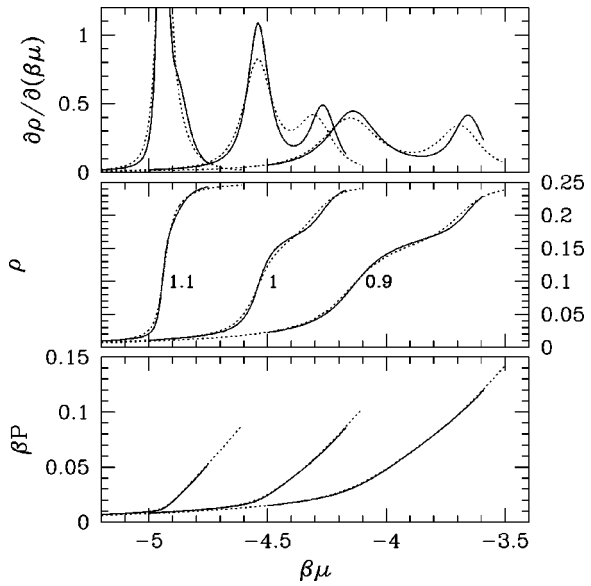

FIG. 8. TM results for the t345 model of Sec. III D. Data for two strip sizes are reported, 10 (dashed line) and 12 (continuous line), and for three isotherms, $\beta\epsilon=0.9,1,1.1$. From top to bottom, results for the reduced compressibility, the average density, and the reduced pressure are shown. Once more, the two-peaked compressibility is informative of the existence of a liquid phase (this phase survives up to $\beta\epsilon\simeq1.1$).

thermodynamic averages both indicate that condensation is strongly discontinuous at $\beta\mu\simeq-4.5$. Moreover, a rather weak first-order (if not even continuous) liquid-solid transition is present at $\beta\mu\simeq-2.5$. The liquid density is within 70% and 85% of the perfect solid density, while the energy per liquid particle varies between -4.4ϵ and -3.9ϵ.

D. Model t345

When the core region embraces second neighbors also, attraction must reach fourth neighbors at least for the liquid to be stable. In fact, the case of a t3 model was already studied in Ref. [13]; there, it was proved that only two phases exist, gas and solid. Moreover, I checked by a series of trial calculations that the liquid is probably absent also in the t34 model for any $\epsilon_3<-\epsilon\equiv\epsilon_4$. In particular, I was never able to observe, either by the TM or by MC simulation, a two-peaked reduced compressibility as a function of $\beta\mu$. Therefore, I promptly move to the t345 model.

For $\epsilon_3=-1.5\epsilon$, $\epsilon_4=-1.2\epsilon$, and $\epsilon_5=-\epsilon$, I plot in Fig. 8 TM results for two strip sizes, $N_x=10$ and 12. N_x must be even in order that the triangular solid, whose density is $\rho=1/4$, fits exactly into the strip. As before, all the states of three consecutive rows are to be counted. For $N_x=12$, the original TM size is 62 996. After collecting states into equivalence classes, this number is reduced eventually to 2840. The two compressibility peaks of a finite three-phase system are found for all $\beta\epsilon$ in the interval 0.5–1. Moreover, the gas-liquid line moves rapidly toward the liquid-solid line as temperature goes down, until they merge together into a single gas-solid transition line at $\beta\epsilon\approx1.2$ and $\beta\mu\approx-5.2$. The latter values thus provide rough estimates of the triple-point coordinates.

In order to obtain further, independent evidence of the stability of the liquid phase, and also more detailed information about its structure, I ran a MC program of the model for two values of $\beta\epsilon$, namely, 1 and 1.1. Numerical data are shown in Figs. 9 and 10 for two lattice sizes, $L=36$ and $L=48$. In Fig. 9, the density histograms and various thermodynamic quantities are plotted for $\beta\epsilon=1$. From this picture, we see that the gas-liquid transition is very smooth. It is hard to say whether a real singularity (second-order transition) occurs in the thermodynamic limit, since no strong size dependence of K_T and C_μ is observed close to $\beta\mu\simeq-4.55$. On the other hand, when $\beta\epsilon=1.1$, condensation is sharply discontinuous at $\beta\mu\simeq-4.93$, as proved in Fig. 10. Actually, $\beta\epsilon=1.1$ appears to be very close to the triple-point temperature. The liquid density is roughly 70–75 % of the perfect solid density, while the energy per liquid particle is between -3.7ϵ and -3.8ϵ.

Perhaps it is worth noting that, in a smaller 24×24 lattice, evidence of a satellite peak at $\rho\simeq0.2$ is found in the density histogram for $\beta\epsilon=1$ (see Fig. 11) which, however, is probably not related to the jamming of the system into a glassy state (this peak is too broad to represent a frozen state). Also, a regular structure where the closest particles occupy fourth-neighbor lattice sites (hence of density 1/7) can be safely excluded. Therefore, the only solution I see is that of a more complex phase behavior in the intermediate-density regime

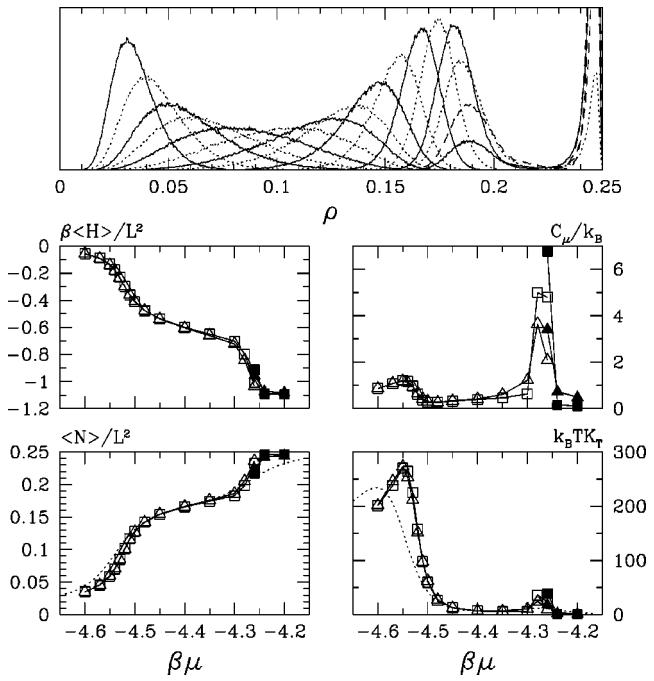

FIG. 9. MC data for the t345 model of Sec. III D, along the isotherm $\beta\epsilon=1$. Above: density histograms for a number of $\beta\mu$ values ranging from -4.6 to -4.2 (the lattice is 48×48). In particular, a dashed line is used for each run of a sequence starting, at $\beta\mu=-4.2$, from a perfect crystal configuration. Units along the y axis are arbitrary. Below: thermodynamic quantities (exact results for a strip of 12 sites are also reported as a dotted line). Two lattice sizes are compared, $L=36$ ($\triangle$) and 48 ($\square$). Values of $\beta\mu$ are the same as for the histograms above. All data points are affected by an error that is smaller in magnitude than the size of the symbols. Full markers refer to simulation runs of the sequence starting on the solid side of the phase diagram. A smooth transition from the gas to the liquid is found at $\beta\mu\simeq-4.53$, while the liquid-solid transition is first order.

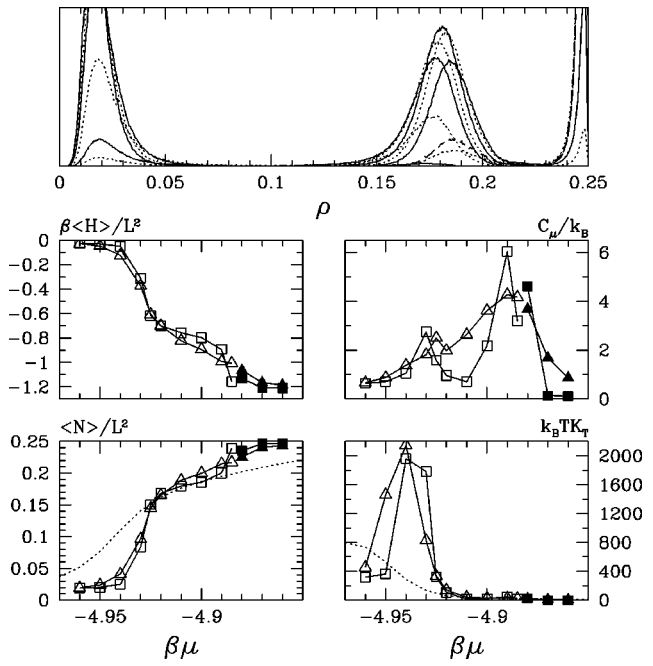

FIG. 10. MC data for the t345 model of Sec. III D, along the isotherm $\beta\epsilon=1.1$. Above: density histograms for a number of $\beta\mu$ values ranging from -4.96 to -4.86 (the lattice is 48×48). In particular, a dashed line is used for each run of a sequence starting, at $\beta\mu=-4.86$, from a perfect crystal configuration. Units along the y axis are arbitrary. Below: thermodynamic quantities (exact results for a strip of 12 sites are also reported as a dotted line). Two lattice sizes are compared, $L=36$ ($\triangle$) and 48 ($\square$). Values of $\beta\mu$ are the same as for the histograms above. All data points are affected by an error that is smaller in magnitude than the size of the symbols. Full markers refer to simulation runs of the sequence starting on the solid side of the phase diagram. Both the gas-liquid and the liquid-solid transitions are now discontinuous.

of the t345 model for small system sizes, which intriguingly recalls the hexatic-phase scenario [3].

E. Model t5678

After a careful investigation of several trial cases, I eventually reached the conclusion that none of the models t5, t56, t567, and t678 has a liquid phase. Finally, I found three phases in the t5678 model for a particular choice of parameters, i.e., $\epsilon_5=-1.15\epsilon$, $\epsilon_6=-1.1\epsilon$, $\epsilon_7=-1.05\epsilon$, and $\epsilon_8=-\epsilon$. Within the TM framework, states of four rows must be enumerated now. N_x is a multiple of 3 in order that the triangular solid ($\rho=1/9$) fits exactly into the strip. Strips of two sizes are considered, $N_x=12$ and $N_x=15$. For the latter case, the number of states is originally 73 131 but, after proper symmetry contraction, it goes down to 2603. To have a taste of the rate at which the TM size increases with N_x, consider that, for $N_x=12$, the two numbers above are ''only'' 7768 and 385, respectively.

The evidence of a liquid is very sharp for the t5678 model; see Fig. 12. Here, TM data are plotted for a number of isotherms in the range $\beta\epsilon=1.4$–1.7. Two clear-cut steps in the density vs chemical potential profile are conclusive evidence for a liquid in this model. Dots superimposed on TM data are MC points for lattices that are very much elongated in the y direction, having 12 and 15 sites in the short direction. Comparison between the two sets of data is good, with the only exception being the solid region where MC sampling is poor. Hysteresis is particularly evident here, as different density and compressibility values are found along the liquidlike and solidlike trajectories.

Surprisingly, the difference in thermodynamic behavior between $N_x=12$ and 15 is enormous, considering that the width of the former is only three sites less than the latter. In particular, the strip of 15 sites is much more reminiscent of the infinite-size behavior. This is particularly transparent in the TM equation of state, which is plotted in Fig. 13. Here, a pair of distinct plateaus is present in each curve, corresponding to gas-liquid and liquid-solid coexistence, respectively. From Figs. 12 and 13, triple-point coordinates are estimated to be $\beta\epsilon\approx2.3$ and $\beta\mu\approx-8$.

A glance at Fig. 14 allows one to appreciate the liquid structure in the t5678 model. This snapshot is taken from a MC run performed at $\beta\mu=-5$ for a 36×36 lattice (periodic boundary conditions are implied). It is clear from this picture that the liquid is an essentially irregular, albeit homogeneous, assemblage of particles containing no crystalline region and, only occasionally, holes large enough to admit another particle. Furthermore, as Fig. 14 well shows, the main difference between the liquid and the solid is not a matter of density, which is pretty much the same for both,

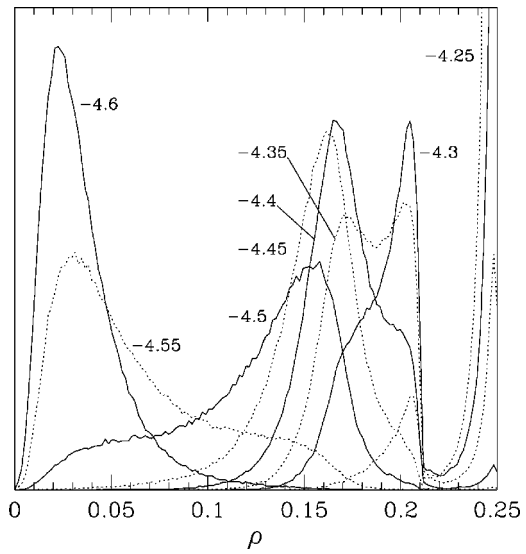

FIG. 11. MC data for the t345 model of Sec. III D, along the isotherm $\beta\epsilon=1$. Density histograms are plotted for a 24×24 lattice. Units along the y axis are arbitrary. Two million MC sweeps are produced at equilibrium for each $\beta\mu$. Runs are performed in sequence, starting from an empty lattice at $\beta\mu=-4.6$. A double-peaked histogram at intermediate densities is indicative of the existence of a more complex liquid structure than in larger system sizes.

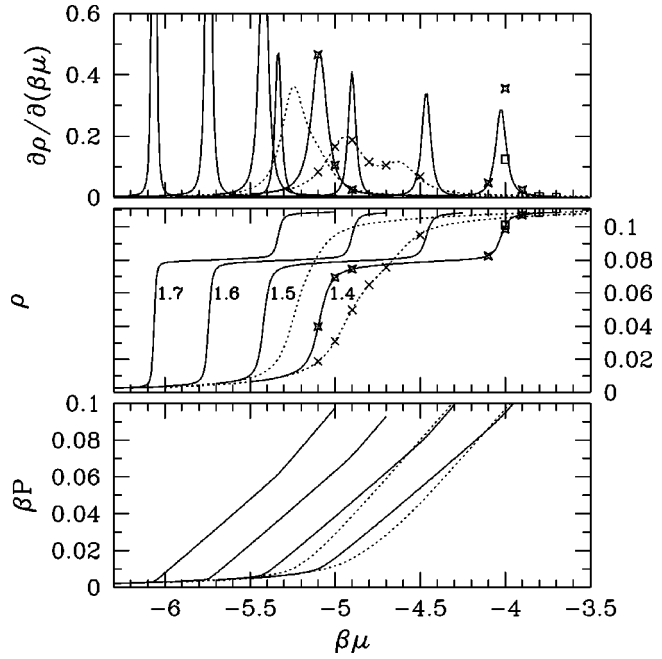

FIG. 12. TM results for the t5678 model of Sec. III E. Here, I show data for two strip sizes, 12 (dotted line) and 15 (continuous line), and for the isotherms at $\beta\epsilon=1.4,1.5,1.6,1.7$. From top to bottom, results for the reduced compressibility, the average density, and the reduced pressure are shown. Symbols are MC data for $\beta\epsilon=1.4$, relative to lattices that are very much elongated in the y direction ($L_y=20L_x$), having 12 and 15 sites in the short direction. These data compare well with TM data. Open squares are for a 15×300 lattice; they were obtained by performing runs in sequence, starting from a perfect crystal at $\beta\mu=-3.7$. All the other points were obtained from simulation runs that were performed in sequence, starting from the empty lattice at $\beta\mu=-5.1$. The existence of two distinct first-order transitions as a function of $\beta\mu$ is well established in this model.

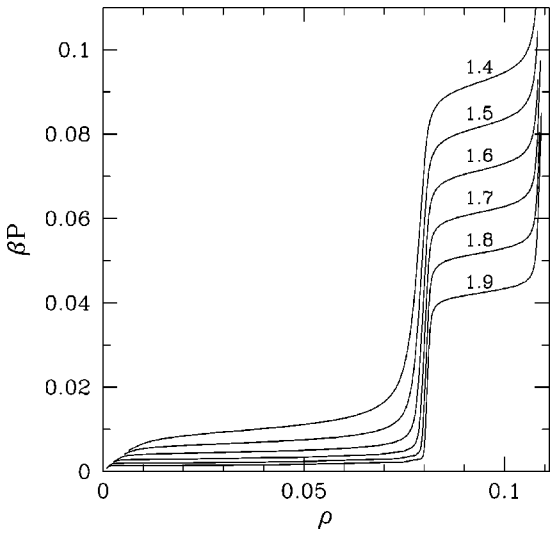

FIG. 13. TM results for the t5678 model of Sec. III E. The strip is $15\times\infty$ here. The exact equation of state (i.e., pressure vs density) is plotted for a number of isotherms, $\beta\epsilon=1.4,1.5,1.6,1.7,1.8,1.9$. Each plateau here corresponds to a region of two-phase coexistence. In particular, note how small is the density interval pertaining to the liquid phase, which is centered around $\rho=0.08$.

but rather of symmetry: While the solid predominantly occupies one out of nine equivalent triangular sublattices, a liquid system is equally distributed among all of them. Finally, I want to stress that, owing to the relatively large core extent in the t5678 model, the structure of the lattice liquid resembles very closely that of a continuous liquid.

Turning to MC simulation, I plot in Fig. 15 a number of density histograms relative to $\beta\epsilon=1.4$, for two lattice sizes, $L=48$ and $L=60$. The gas-liquid transition is clearly first order here, with a liquid peak that, in the 60×60 lattice, is centered at about 70% of the maximum density. Upon increasing $\beta\mu$ further, a spurious transition to a glassy state finally occurs. This can be seen from the drop of the MC acceptance ratio close to $\beta\mu\simeq-4.8$, which is the point where the system density jumps from one peak to the other. This ''glass transition'' can be delayed substantially in μ if the latter is made to increase in small enough steps.

For $L=48$, only one peak is present in the histogram, whose likely character is that of a glass (this is because of the small peak width, which is indicative of a frozen structure). The absence of the liquid peak might well be due to the proximity of the liquid density to the random-sequential-addition threshold for the same L, i.e., to the existence in phase space of a huge number of glass configurations in the close neighborhood of the liquid basin. Anyway, this is a sporadic finite-size peculiarity that is already absent in a 60×60 system and, probably, also in larger lattices.

In Fig. 16, I plot thermodynamic averages for the same two sizes. For $L=60$, the energy per liquid particle is about -3.1ϵ. The pseudotransition to the glass is now fairly evident; it is marked by a small jump in all thermodynamic quantities at $\beta\mu\simeq-4.8$. I also notice that, upon reducing $\beta\mu$ to -4.3, the solid jumps to a disordered state which is glassy, not liquid.

Finally, I have checked whether the absence of a genuine liquid in the 48×48 system should perhaps be ascribed to the

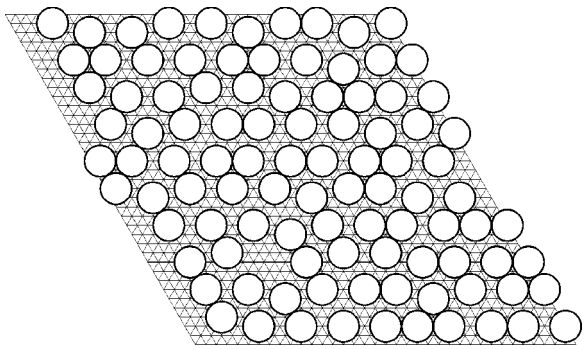

FIG. 14. MC snapshot of a liquid configuration in the t5678 model of Sec. III E, for $\beta\epsilon=1.4$ and $\beta\mu=-5$ (the lattice is 36×36). The average density at this $\beta\mu$ is 0.0737. The fine grid on the background is the triangular lattice (periodic boundary conditions are implied). Due to the relatively small ratio between the lattice constant and the particle diameter, the discreteness of the host space is hardly appreciated from looking only at the particles.

MC algorithm being used. With this aim, I ran a modified MC program that, in addition to grand canonical moves, also allows for ''canonical'' moves, i.e., attempts for a particle to diffuse toward a nearest-neighbor site in the triangular lattice. As a matter of fact, the new data points are indistinguishable from the previous ones. This makes the impression

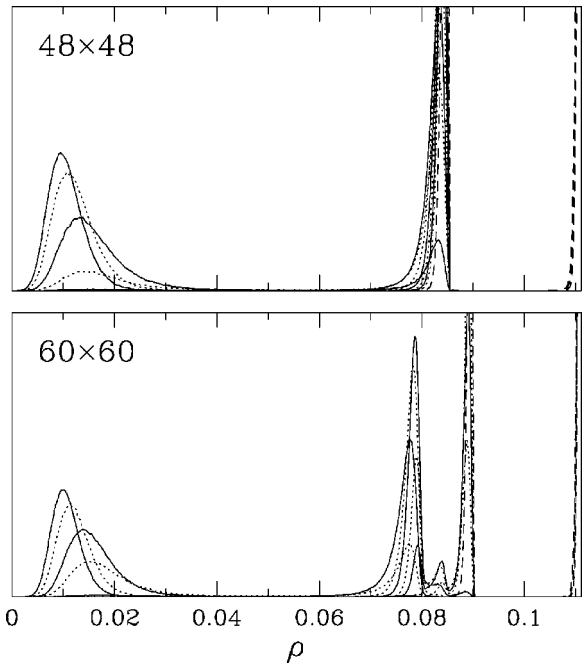

FIG. 15. MC data for the t5678 model of Sec. III E, along the isotherm $\beta\epsilon=1.4$. Density histograms for two lattices are plotted for a number of $\beta\mu$ values in the range between -5.25 and -3.7 (these values are $-5.25,-5.2,-5.14,-5.12,-5.1,-5,-4.9,-4.8,-4.7,-4.6,-4.3,-4.1,-3.9,-3.7$). In particular, I have used a dashed line for any run of a sequence starting at $\beta\mu=-3.6$ from a perfect crystal and ending at $\beta\mu=-4.4$ in a glassy state (see also Fig. 16). Units along the y axis are arbitrary. After condensation, the 48×48 lattice immediately gets trapped into a glassy state while, on the other hand, the 60×60 lattice shows a genuine liquid structure around $\beta\mu=-5$ ($\rho\simeq0.078$; it then also becomes glassy at $\rho\simeq0.089$).

stronger that the equilibrium liquid state is really suppressed in a 48×48 lattice.

IV. DISCUSSION

As well as their intrinsic value, the above results also provide a way to build up a 3D lattice-gas system with a realistic surface. As discussed in the Introduction, a simplified lattice model of a 3D system with both solidlike (discrete) and liquidlike (continuous) features can be useful for a deeper understanding of many surface phenomena.

For instance, as temperature goes up, the (111) surface of an argon crystal first undergoes a preroughening (PR) transition at approximately 85% of the melting temperature. There are solid-on-solid (SOS) lattice models that deal with this phenomenon rather accurately [14,8]. For temperatures above the PR transition and below roughening, the topmost surface layer is roughly half occupied. Hence, liquidlike diffusion has a chance to grow substantially in the surface layer. It is believed that the onset of surface melting is in fact associated with a strong enhancement of diffusive processes which, however, cannot be treated in terms of a SOS model. Therefore, in order to understand the relevance of PR to the beginning of surface melting, a description in terms of a model that embodies both discrete and continuous features is in order. To this end, a 3D Potts model has recently been proposed [9]. In view of the results of Sec. III, a more realistic description of the same phenomenon, still in terms of a lattice model, can now be advanced.

Take, as an example, the t345 model of Sec. III D. The nearest-neighbor distance in the perfect solid is $2a$, i.e.,

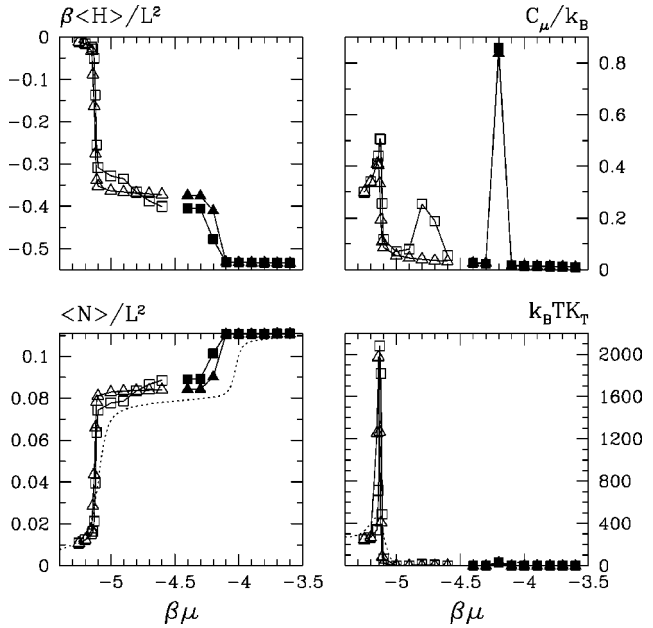

FIG. 16. MC data for the t5678 model of Sec. III E, along the isotherm $\beta\epsilon=1.4$. Thermodynamic quantities for two lattices, $L=48$ (△) and 60 (□), are compared, along with exact results for a strip of 15 sites, here reported as a dotted line. All data points are affected by an error that is smaller in magnitude than the size of the symbols. Full markers refer to simulation runs of the sequence starting on the solid side of the phase diagram. Both the gas-liquid and the liquid-solid transition are strongly first order. A pseudotransition from the liquid to a glass is also present in the larger lattice.

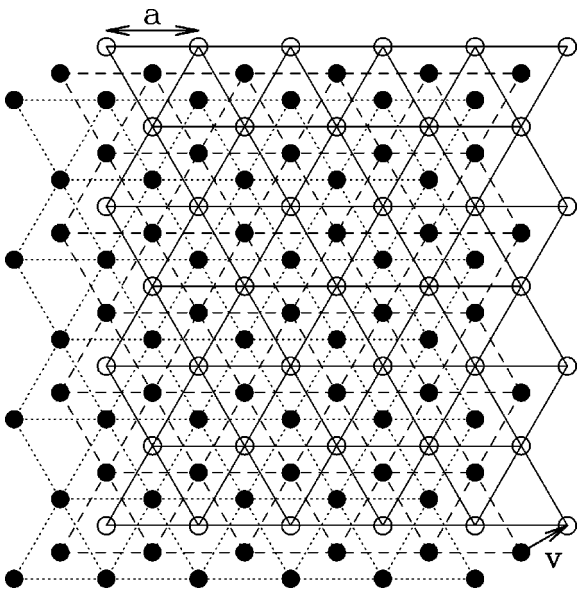

FIG. 17. The 3D lattice shown here is made of a stack of triangular planes, each obtained from the plane below by application of a suitable **v** translation. This lattice can host close-packed fcc configurations of particles of either size $2a$ (one lattice plane being occupied in every two) or $3a$ (one occupied plane in every three).

twice the triangular-lattice parameter. Now suppose a stack of triangular lattices is piled up together, in such a way that each plane is displaced by $\mathbf{v}=(1/2,\sqrt{3}/6,\sqrt{6}/3)a$ from the one below (see Fig. 17). Then, a perfect fcc crystal oriented along [111] is obtained by filling one lattice plane of every two with spherical particles of diameter $2a$, thus giving rise to a system with an overall density 1/8 of occupied sites.

Each site in this 3D lattice has twelve first neighbors around it. More generally, any of the sites has neighbors at all integer square distances. In particular third, fourth, and fifth in-plane neighbors will correspond to fourth, seventh, and ninth 3D neighbors, respectively (note, however, that there are also out-of-plane seventh and ninth neighbors).

It is now easy to construct a 3D potential which, when projected on 2D, gives back the same t345 parameters of Sec. III D. One possibility is to take an attractive potential that is a linear function of the square distance in the range between $(2a)^2$ and $(3a)^2$, such that the strength of attraction between fourth neighbors is 50% larger than that between ninth neighbors, equal in turn to ϵ. Moreover, an infinite repulsion is assumed for distances below $2a$, and no interaction at all beyond $3a$. The occurrence of a liquid in this model can be guessed from the criterion that was mentioned in the Introduction (in fact, the width of the attractive well is equal to the particle radius, that is to say, larger than one-third of the diameter). If the liquid were altogether absent, one could anyway supply the t345 model with a longer attractive tail (which makes the liquid phase more robust) until a stable liquid was obtained also in 3D. The resulting lattice model would provide a natural tool for studying the interplay between PR and surface melting, thus competing in accuracy with a system of Lennard-Jones particles [15]. In particular, at variance with a continuous system, a lattice system would permit a neater description of PR (i.e., beyond the SOS approximation) and a better investigation of the correlation existing between PR and the process of sublattice disordering in the surface layer.

V. CONCLUSIONS

In the present paper, conclusive evidence has been provided of the existence of an isostructural, gas-liquid phase transition in three different models of a homogeneous and isotropic 2D lattice gas on the triangular lattice. In all cases, the solid structure is triangular as well. From this study, I draw the conclusion that, whatever the extent of the hard-core region, there is room for a liquid in a lattice system provided that the attractive tail of the potential is sufficiently longer than the core length, the more so the smaller the core (see Fig. 1, caption).

Next, I have presented a 3D lattice-gas model which I propose to be a natural candidate for simulating problems in surface physics where both discrete and continuous degrees of freedom are expected to play a role. In the near future, I plan to use such a model with the view of gaining a better (i.e., microscopic) understanding of the onset of surface melting in a rare-gas (111) solid surface.

[1] For a review, see L. K. Runnels, in *Phase Transitions and Critical Phenomena*, edited by C. Domb and M. S. Green (Academic, London, 1972), Vol. 2.

[2] In particular, the standard ferromagnetic Ising model on the square lattice provides also a model of the gas-liquid transition, whereas the Ising antiferromagnet more properly furnishes a caricature of the gas-solid transition. Inclusion of further-than-nearest-neighbor interactions leaves the phase behavior qualitatively unaltered (see Ref. [6] for a thorough discussion of this point).

[3] A classic review article is K.J. Strandburg, Rev. Mod. Phys. **60**, 161 (1988). Recently, hints of a hexatic phase have been found in a number of simple-fluid systems: see, for instance, K. Chen, T. Kaplan, and M. Mostoller, Phys. Rev. Lett. **74**, 4019 (1995); A. Jaster, Phys. Rev. E **59**, 2594 (1999).

[4] J. Orban, J. Van Craen, and A. Bellemans, J. Chem. Phys. **49**, 1778 (1968).

[5] R. Kikuchi, J. Chem. Phys. **68**, 119 (1978); R. Kikuchi and J.W. Cahn, Phys. Rev. B **21**, 1893 (1980); G. An and M. Schick, *ibid.* **39**, 9722 (1989).

[6] D. Poland, Phys. Rev. E **59**, 1523 (1999).

[7] P. Bolhuis and D. Frenkel, Phys. Rev. Lett. **72**, 2211 (1994).

[8] See, e.g., S. Prestipino and E. Tosatti, Phys. Rev. B **59**, 3108 (1999), and references therein.

[9] E.A. Jagla, S. Prestipino, and E. Tosatti, Phys. Rev. Lett. **83**, 2753 (1999).

[10] For a simple introduction to the TM method, see, e.g., T. L. Hill, *Statistical Mechanics* (Mc Graw-Hill, New York, 1956).

[11] L.K. Runnels and L.L. Combs, J. Chem. Phys. **45**, 2482 (1966).
[12] L.K. Runnels, L.L. Combs, and J.P. Salvant, J. Chem. Phys. **47**, 4015 (1967).
[13] L.K. Runnels, J.R. Craig, and H.R. Streiffer, J. Chem. Phys. **54**, 2004 (1971).
[14] S. Prestipino, G. Santoro, and E. Tosatti, Phys. Rev. Lett. **75**, 4468 (1995).
[15] F. Celestini, D. Passerone, F. Ercolessi, and E. Tosatti, Phys. Rev. Lett. **84**, 2203 (2000).